PROCEEDINGS OF SCIENCE
ONLINE ICRC 2021 THE ASTROPARTICLE PHYSICS CONFERENCE Berlin | Germany
37th International Cosmic Ray Conference 12–23 July 2021

SiPM Based Imaging Camera for 4m Class Telescope

V. R. Chitnis,[a,*] **S. S. Upadhya,**[a] **K. S. Gothe,**[a] **S. Duhan,**[a] **S. K. Rao,**[a] **B. B. Singh,**[a] **M. Ranjan,**[a] **N. K. Parmar,**[a] **A. Chatterjee,**[a] **R. L. Deshmukh,**[a] **P. Dorjey,**[a] **N. Dorji,**[a] **A. P. K. Kutty,**[a] **B. K. Nagesh,**[a] **V. A. Nikam,**[a] **S. R. Patel,**[a] **A. Roy,**[a] **M. N. Saraf,**[a] **A. Sarkar,**[a] **P. Verma,**[a] **K. K. Yadav,**[b] **N. Chouhan,**[b] **V. K. Dhar,**[b] **P. Chandra**[b] **and K. Venugopal**[b]

[a] *Department of High Energy Physics, Tata Institute of Fundamental Research, Homi Bhabha Road, Colaba, Mumbai 400 005, INDIA*

[b] *Astrophysical Sciences Division, Bhabha Atomic Research Centre, Trombay, Mumbai 400 085, INDIA*

E-mail: vchitnis@tifr.res.in

In last few years, SiPMs have emerged as a viable alternative to PMTs used in the imaging atmospheric Cherenkov telescopes. In addition to their higher photon detection efficiency, SiPMs provide attractive features like possible increase in observation duty cycle owing to their safe operation under partial moonlight conditions. Design and development of 256 pixel SiPM based camera for a 4m class Cherenkov telescope is currently at an advanced stage. This camera is proposed to cover a field of view of $5^\circ \times 5^\circ$, with a pixel size of $\sim 0.3^\circ$. The camera being developed, is planned to be mounted in the focal plane of one of the vertex elements of TACTIC telescope system which is currently operational at Mt Abu, in the north-western part of India. The associated camera electronics will also be mounted in focal plane of telescope behind the SiPM pixels. The camera will have modular structure, with each module consisting of 16 pixel sensors and the associated front end electronics. The signal generated from the pixels on registration of a Cherenkov event will be passed to "back-end" electronics for trigger generation, digitization @1GSPS and the subsequent data recording. A 16-pixel prototype module has already been developed and tested in our laboratory. A "mini- camera" consisting of 64 pixels has also been assembled and is currently at advanced stage of testing. After completion of the successful testing of the "mini-camera", field tests at the telescope site will be conducted. Salient features of the SiPM based camera, results from the tests conducted by us and status report will be presented.

37th International Cosmic Ray Conference (ICRC 2021)
July 12th – 23rd, 2021
Online – Berlin, Germany

*Presenter

PoS(ICRC2021)719

1. Introduction

During last decade, SiPMs or Silicon Photomultipliers have emerged as a viable alternative to PMTs for use in imaging atmospheric Cherenkov telescopes (IACTs). SiPMs have several attractive features. In addition to characteristics like fast response and high gain, which they share with PMTs, SiPMs have several advantages like higher photon detection efficiency, well-resolved photoelectron spectrum, etc. SiPMs are compact, light-weight, mechanically robust, and are insensitive to a magnetic field. Also, they need lower bias voltage (~ 30-70 volts), whereas PMTs need a voltage of the order of kV. Another important advantage of SiPMs is that they can be operated in a bright environment safely. So it is possible to increase the observation duty cycle by operating the telescope partially in the moonlit part of the night or during twilight. One telescope, First G-APD Cherenkov Telescope (FACT), with 1440 pixel SiPM based camera is operational for almost ten years now [1]. Several blazars have been observed with this telescope. Apart from establishing usage of SiPMs as sensors for IACTs, this telescope has also demonstrated an increase in duty cycle compared to PMT-based IACTs [2]. Even though SiPMs have several good features, they also have few disadvantages like higher cross-talk and temperature dependence of gain. It is necessary to take corrective measures, particularly for the temperature dependence of gain, while designing SiPM based camera. In the following sections, we describe the SiPM based camera we are developing for small size telescope. This telescope will be dedicated to observations of blazars. Design details of this camera, current status, and plans for installation are described in subsequent sections.

2. Design Features of Camera

SiPM based camera is being designed for 4m class telescope. It will be installed on one of the vertex elements of TACTIC (TeV Atmospheric Cherenkov Telescope with Imaging Camera) telescope operational at Mt. Abu, in the north-western part of India. TACTIC is an array of four telescopes, with PMT based camera installed on the central telescope. This telescope is called imaging element and is operational for last twenty years. Telescope structures of three vertex elements situated at corners of a triangle are identical to the imaging element. Each of these telescopes consists of 34 glass spherical mirror facets with a total light collector area of 9.5 m^2 and focal length of nearly 4m. Further details about TACTIC can be found in [3].

The SiPM camera will consist of 256 pixels of size $0.3^\circ \times 0.3^\circ$ with a total field of view of $5^\circ \times 5^\circ$. Each pixel sensor will consist of 4×4 array of Hamamatsu SiPMs with the size of each element of the array being 3 mm × 3 mm. Array elements are referred to as sub-pixels in this paper. Hollow light concentrator with square entry (21 mm × 21 mm) and square exit (12.4 mm × 12.4 mm) will be mounted in front of pixel sensors. Entire electronics including front end and back end electronics will be mounted behind the pixel sensors in the focal plane of the telescope.

Design parameters for the camera are decided considering telescope geometry as well as using simulations of extensive air showers initiated by gamma rays and cosmic rays. Based on simulations, the optimum dynamic range for the camera is decided to be at least upto 1500 photo-electrons. Timing resolution of 1 ns is desirable for recording Cherenkov pulse profiles. As this telescope is supposed to be a monitoring instrument with a longer duty cycle, the operation will be carried out not only on dark nights, but also during twilight as well as moonlit part of the night. The night sky background rate for the dark night is estimated to be about 93 MHz/pixel based on measurements. Under moonlit conditions background rate could be quite high, as high as 10 GHz/pixel. The event rate is expected to be 20-30 Hz on dark nights. So electronics should handle event rates at least up to 100 Hz. Entire electronics will be mounted in the focal plane. The maximum weight of the camera that can be safely supported by the mechanical structure of the telescope is ~ 100 kg, putting a limit on the weight of the camera. Also, power consumption should be limited within 500 W to ensure safe operation with a simple air cooling system.

Various parts of the camera are shown schematically in Fig. 1. Camera front end will have a modular structure with each module consisting of 16 pixel sensors and associated front end electronics. There will be 16 such modules. Light concentrators will be mounted in front of SiPMs. Back end part of the camera will also be modular in structure consisting of digitizer modules, data concentrator module and control and trigger module.

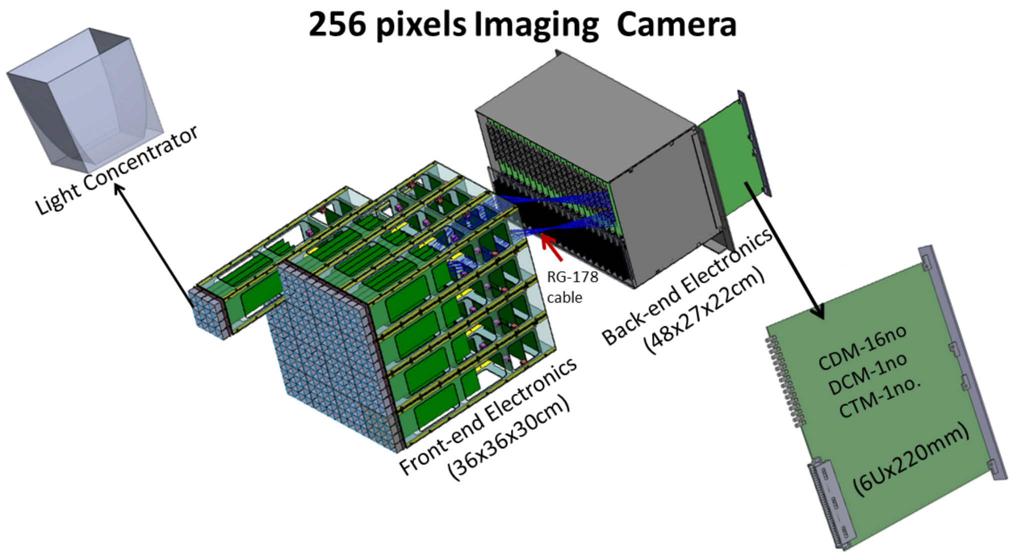

Figure 1: Schematic representation of various subsystems in camera

3. Camera Subsystems

Various subsystems of the camera are discussed below.

3.1 Front End Electronics

Front end electronics of the camera is divided into 16 identical modules called pixel cluster modules, each catering to 16 pixels. Each module consists of a sensor mount board, four 4-pixel pre-amplifier boards, two 8-pixel bias supply cards and a low voltage supply card. SiPM gain varies as a function of temperature because of the temperature dependence of breakdown voltage. It is necessary to compensate for this effect by maintaining constant over-voltage above breakdown voltage. SiPMs used in this camera typically need a bias voltage of about 55 V and breakdown voltage varies with temperature at the rate of 54 mV/°C. Bias supply designed is based on DC/DC converter HV80 from AiT instruments and it provides voltage in the range of 0-80 V with 4 mA load with a minimum step size of 5 mV. Temperature dependence of gain is studied using an environmental chamber over the temperature range of -20 to +30°C. This dependence is parameterised and used by micro-controller based bias supply. Micro-controller reads temperature from sensors mounted near SiPMs and applies correction to the bias voltage. Fig. 2 shows graph of output pulse height vs temperature without and with temperature compensation. A remarkable reduction in gain variation from 97% to 3% is achieved over the temperature range of -20 to +30°C.

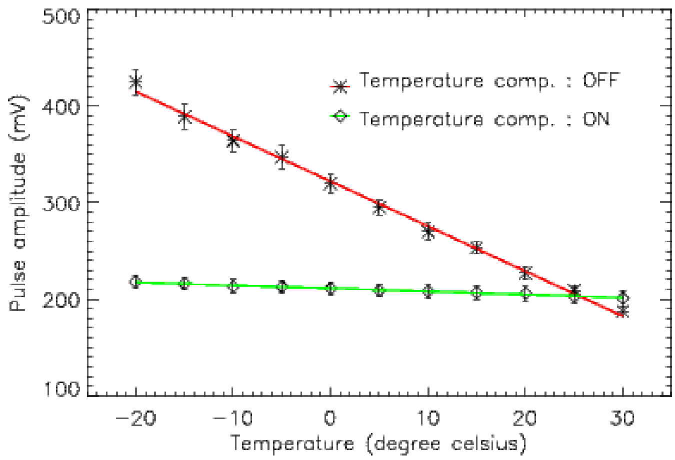

Figure 2: Compensation for variation of SiPM gain with temperature

Pulses from SiPMs are given to the pre-amplifier. Design goals for pre-amplifier are quite demanding. Firstly, SiPMs have huge capacitance at the output which scales as sensor area. The capacitance of 3 mm × 3 mm sub-pixel in each pixel sensor is 320 pF and this appears at the input of the pre-amplifier. Hence in order to limit the decay time of the output pulse, a very low impedance amplifier is needed, which is achieved by using transistor based Trans-Impedence Amplifier (TIA). Input impedance of TIA is 6 ohms and gain corresponds to 0.64 mV/micro-amps. As the addition of all sub-pixel pulses to form a pixel pulse before TIA stage results in even higher capacitance at TIA input, amplification of sub-pixel pulses and subsequent addition would be a better option. But this increases TIA electronics by a factor of 16. Hence, as a trade-off, 8 sub-pixel pairs are formed, which are then amplified and added. For single photo-electron (pe) input TIA produces an output pulse of 8 mV peak amplitude, with the rise time of 6 ns and base width of 80 ns, for over-voltage of 3 Volts. Considering the large background rate from the night sky, a significant pulse pile-up is expected. In order to reduce this effect, TIA outputs from sub-pixel pairs are shortened to 20 ns width using pole-zero cancellation technique. Shaped outputs from 8 sub-pixel pairs are then added using a summing amplifier. TIA, shaper and summing amplifier together constitute pre-amplifier. Components in these circuits are chosen carefully considering desired features like low power, low noise and high bandwidth. Also there is a provision to enable and disable individual sub-pixels for in-situ calibration of the single pe gain of a pixel. Required dynamic range upto 1500 pe is covered by amplifying pixel signal from pre-amplifier using dual gain stages in parallel, viz. low and high gain.

Performance of the pre-amplifier was tested using a pulsed laser system in black-box with VME based digitizer. Fig. 3a shows pulse charge distribution clearly showing the separation between pedestal, single pe, 2 pe pulses etc. Fig. 3b shows linearity of the low gain channel over the pulse amplitude range upto 1600 pe.

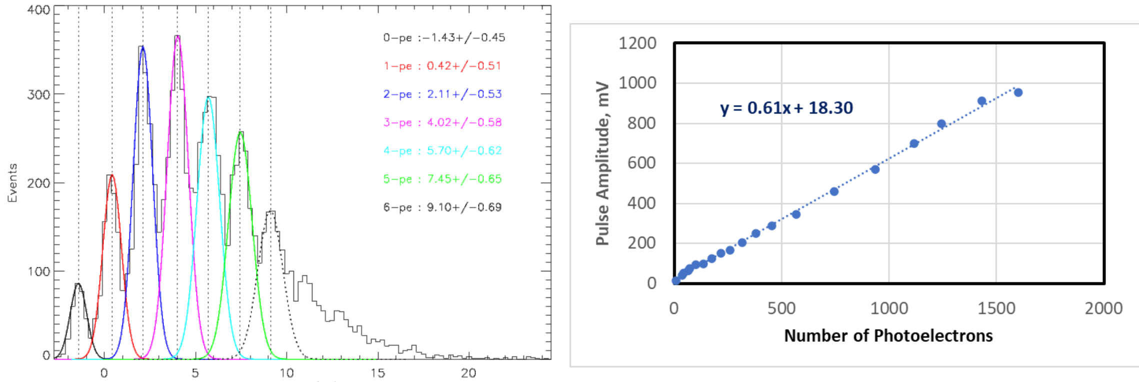

(a) **(b)**

Figure 3: (a) Pulse charge distribution, (b) Linear response of low gain channel

Apart from bias supply and pre-amplifier cards, there is a low voltage power supply card in front end electronics giving required low voltages to various cards.

3.2 Back End Electronics

Amplified pulses from low gain and high gain channels are further processed in back end electronics. It consists of 16 cluster digitizer modules, control and trigger module and data concentrator module mounted in a crate behind front end electronics or cluster of 16 pixel cluster modules. Digitizer modules are based on analog Domino Ring Sampler or DRS4 chips, which sample pulse profiles with the rate of 1 GSPS. Each digitizer module houses 4 mezzanine digitizer boards to digitize total of 36 channels catering to low gain and high gain outputs from 16 pixels along with 4 calibration signals. On receipt of the trigger, sampling is halted after pre-determined delay and information in the region of interest (ROI) is digitised using 14 bit ADC at 33 MHz rate. Digitizer modules have comparators to generate first level trigger or pixel trigger with a programmable threshold. Also FPGAs are incorporated in digitizer modules for multiplexed digitization, for recording ROI, for setting threshold, pixel enable/disable etc. Data from digitizer modules are transmitted over the serial link to the data concentrator module as segmented event packets for corresponding 4 pixels.

The next module in back end electronics is the control and trigger module which has control section and trigger section. The control section is responsible for sending control / configuration / initialization data to all other back-end modules and recording monitoring data from all digitizers. FPGA in control and trigger module interfaces to all other modules using customised SPI (cSPI) protocol over back-plane of the crate and also with remote control room over Ethernet for communication and data transfer. The trigger section receives 64 pre-trigger signals from 16 digitizer modules, generates the final trigger and then sends the final trigger signal to digitizer modules to initiate data recording. It also generates event number and time stamp synchronised with GPS and sends them to digitizer modules over a common serial link. This module also provides a 10 MHz clock signal to all modules for synchronization.

Two types of triggers have been incorporated in the trigger section : NCT or non-collinear triplets and 4NNB or 4 nearest neighbour pixels crossing a programmable threshold in terms of number of pes. A coincidence window of 5 or 10 ns is used. As triggering pixels may or may not be fully contained in one digitizer module, trigger generation goes through few steps. Each digitizer module generates four pre-trigger outputs which are sent to the control and trigger module : If the trigger condition is satisfied within a digitizer module, it generates a full trigger which is sent to the control and trigger module for the generation of a final trigger. Each digitizer module also generates two-fold and one-fold outputs if boundary pixels cross the threshold and are likely to generate the trigger in combination with boundary pixels of neighbouring digitizer modules. The fourth output is a pixel hit pattern sent over a serial link using which control and trigger module can resolve valid boundary pixels. If the trigger condition is satisfied, the control and trigger module sends a final trigger followed by a validation signal to all digitizer modules and then all digitizer modules send data packets consisting of pulse profiles in ROI to data concentrator module. Then data concentrator module sends data to the remote PC over two 1 GbPS Ethernet links. This module consists of two identical circuits, each one catering to data from half of the camera. Data throughput rate upto 100 MBPS is achieved. Fig 4 shows typical pulse recorded with high gain channel during laboratory tests under laser illumination with entire electronics.

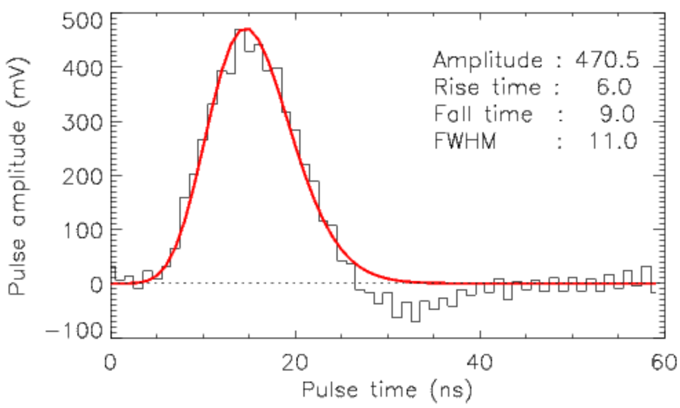

Figure 4: Typical pulse recorded under laser illumination

3.3 Software and Data Format

Data is recorded in binary format. Assuming 50 ns ROI, the data size for 256 pixels will be 65 kbytes per event and the maximum event rate that can be handled would be about 1200 Hz. For event rate of 50 Hz, about 11.6 GB of data will be recorded per hour. Data is later converted from binary format to ROOT format. Interactive Qt-ROOT based GUI is developed to control camera operation and monitor various parameters during the run.

The software consists of two parts : First part is the software installed on camera which consists of bias control and monitoring system with micro-controller based 32 Bias cards connected with single Raspberry-Pi through cSPI, control/trigger and digitizer modules built over NIOS soft processor and VHDL coded data concentrator module to collect data from all digitizers and send it to the control room over two Ethernet links. Second part of the software is control room software consisting of data base storing calibration and configuration data, bias server for front end control and biasing, main console for overall camera control and monitoring, event builder for building events from segmented data packets. Also there is a NAS system which is a repository to store all data. Analysis packages retrieve data from repository during on-line and off-line analysis.

3.4 Other Subsystems

There is a plan for in-situ calibration setup consisting of UV-blue laser, neutral density filters and diffuser, which will be mounted in the focal plane of the telescope which will be used for SiPM gain calibration, checking for linearity of gain etc. Also calibration system consisting of LEDs will be mounted on the camera lid. Laboratory setup for SiPM characterisation consisting of pulsed LED, beam splitter, reference detector and diffuser is assembled. To study the temperature dependence of some of the characteristics environmental chamber is used. Using this setup various measurements are carried out on a number of SiPMs including dark and cross talk rates, breakdown voltage and its temperature dependence, absolute gain and its linearity, sub-pixel pulse shapes and their addition in pixel pulses.

4. Expected Performance Parameters

SiPM camera will be installed in the focal plane of one of the vertex elements of TACTIC and will be tested thoroughly at Mt Abu and later it will be shifted to Hanle in Himalayas. Performance parameters are estimated for Mt Abu location simulating showers initiated by gamma rays and protons using CORSIKA package [4]. Cherenkov photon distribution generated with CORSIKA is traced to the reflector and later to the camera plane. Various parameters like night sky background rate of about 93 MHz/pixel, light concentrator efficiency, single pe pulse shape from SiPM and trigger criteria are taken into consideration. For trigger condition of at least 10 pe in NCT, the expected cosmic ray trigger rate is about 22 Hz and the energy threshold at trigger level is expected to be $\sim$ 510 GeV. With Hillas parameterisation of simulated images, static and dynamic supercuts as well as random forest methods were applied for gamma-hadron segregation. Based on random forest, for optimum conditions, 5σ detection sensitivity for Crab like sources corresponds to an observation duration of about 104 minutes. Eventually telescope will be installed at Hanle and for this location, because of the higher altitude (4270 m asl vs 1300 m asl for Mt Abu), the energy threshold is expected to reduce to about 220 GeV.

5. Current Status and Future Plans

The 64-pixel mini-camera or setup consisting of four 16-pixel modules along with back end electronics has been assembled and being tested in the laboratory (see Fig. 5). More than 100 SiPMs have been characterised as of now. Light concentrators have been manufactured and tested. Housing for camera is under development. After completion of laboratory tests we plan to test mini-camera at Mt Abu by October-November this year. Parallelly work on the remaining modules will be initiated and the entire camera is expected to be ready for tests by end of 2022. After completion of tests at Mt Abu telescope will be shifted to Hanle and will be dedicated to monitoring of blazars. It will complement 21m diameter MACE telescope which is at an advanced stage of commissioning at Hanle [5]. It is possible to operate this telescope in synergy with FACT and have longer duration coverage for blazars.

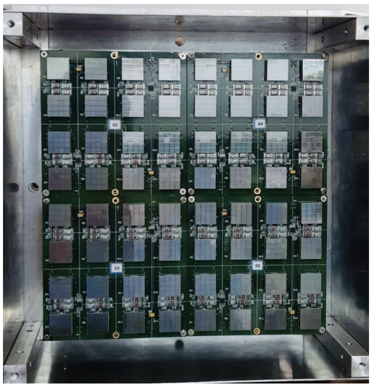

(a)

(b)

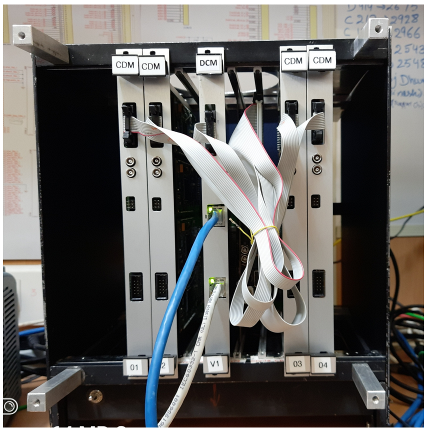

(c)

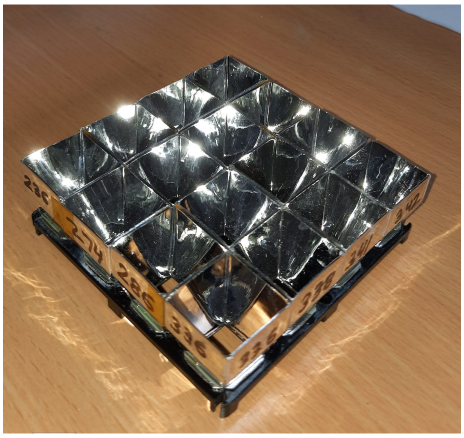

(d)

Figure 5: (a) Front view and (b) side view of mini-camera, (c) back end electronics mounted in crate, (d) Light concentrator assembly

References

[1] H. Anderhub et al., Journal of Instrumentation, **8**, P06008, 2013

[2] D. Dorner et al., Proceedings of the 34th ICRC (ICRC2015), id. 704, 2015

[3] R. Koul et al., Nuclear Instruments and Methods in Physics Research, **A 578**, 548, 2007

[4] D. Heck et al., CORSIKA: a Monte Carlo code to simulate extensive air showers, Report number: FZKA-6019, 1998

[5] C. Borwankar et al., Astroparticle Physics, **84**, 97, 2016